European Journal of Cardio-Thoracic Surgery 51 (2017) 432–441
doi:10.1093/ejcts/ezw347 Advance Access publication 24 December 2016

ORIGINAL ARTICLE

Cite this article as: Berdajs D, Mosbahi S, Strano F, Forro Z, Burki M, von Segesser LK. Impact of synthetic elements on aortic root haemodynamics: computed fluid dynamics of aortic root reconstruction and valve reimplantation. Eur J Cardiothorac Surg 2017;51:432–41.

Impact of synthetic elements on aortic root haemodynamics: computed fluid dynamics of aortic root reconstruction and valve reimplantation

Denis Berdajs[a,b,*], Selim Mosbahi[a], Francesco Strano[a], Zalan Forro[c], Marco Burki[a] and Ludwig K. von Segesser[a]

[a] Department of Surgery and Anesthesiology, Cardiovascular Research, University Hospital Lausanne, Lausanne, Switzerland
[b] Department of Cardiac Surgery, University Hospital Basel, Basel, Switzerland
[c] Swiss Federal Institution of Technology Zürich, Zürich, Switzerland

* Corresponding author. Department of Cardiac Surgery, University Hospital Basel, Spitalstrasse 21, Basel CH-4031, Switzerland. Tel: +41-61-3287180; fax: +41-61-2657324; e-mail: denis.berdajs@bluewin.ch (D. Berdajs).

Received 16 March 2016; received in revised form 14 September 2016; accepted 19 September 2016

Abstract

OBJECTIVES: The aim was to evaluate the impact of the aortic valve reimplantation (David) and of the aortic root (AoR) remodelling (Yacoub) on the AoR haemodynamics.

METHODS: In an experimental setup where the clinical scenario of Yacoub, ($n = 5$, domestic pig) and of David ($n = 5$, domestic pig) procedure was performed in each AoR, six high-fidelity (200 Hz) sonomicrometric crystals were implanted. Crystals were positioned at three commissures with their projection at the root base. In post-measurement processing 3D deformation of both AoR was determined and used for computed fluid dynamic modelling in order to evaluate pressure, velocity and shear stress profiles.

RESULTS: In David AoR: high pressure (> 150 mmHg) and low to moderate shear stress (0–30 Pa) were found from the period of isovolemic contraction to the closure of the aortic valve. At mid diastole pressure augmentation (> 120 mmHg) a low shear stress (0–10 Pa) was registered at the leaflets, three commissures, and intervalvular triangles. In Yacoub AoR: high pressure (110–130 mmHg) with moderate low shear stress (0–30 Pa) was only registered at isovolemic contraction.

CONCLUSION: The results show that haemodynamic conditions following a David procedure have a less favourable pattern as compared to a Yacoub AoR. In David AoR, high pressure and low shear stress are present during 2/3 of the cardiac cycle, whereas in Yacoub root, these conditions are present only for a short period of isovolemic contraction.

Keywords: Aortic root • Aortic valve • Computed fluid dynamics

INTRODUCTION

Aortic root (AoR) haemodynamics is complex and is determined by precisely defined time- and space-related deformation of the AoR components. Analysis of time-related 3D geometry demonstrates that the AoR changes from a tilted-cone-like architecture during diastole to a straight cylinder shape during ejection. This formation later provides a straight alignment between the left ventricular outflow tract (LVOT), AoR, and ascending aorta, and as such provides an open path for large-volume flow during ejection with minimal resistance and shear stress [1, 2]. Considering this it is easy to understand that any deviation of the natural AoR architecture results in malfunction of the AoR as a unit.

Current AoR reconstructive procedures aim to restore the natural configuration of the AoR in order to regain the competent leaflet function. Currently, two surgical techniques are in general use, the aortic valve reimplantation (David) and the AoR remodelling (Yacoub) technique [3, 4]. AoR remodelling is suggested as providing more physiological valve movement with the creation of neo sinuses of Valsava. It does not, however, address late dilatation of the AoR base, as is the case with Marfan syndrome [3, 5, 6]. In contrast, in the reimplantation technique, the aortic valve is inserted into a straight tube, and as thus provides the stabilization effect for the all AoR elements. This has been shown to be protective for late aortic annulus dilatation [7, 8]. Although both methods are considered to be standard surgical techniques in many clinical scenarios, not all facets of each procedure have been evaluated in term of influence on AoR performance.

The aim was to evaluate and compare the impact of AoR remodelling and reimplantation technique on AoR haemodynamics. For this purpose, a previously defined numerical approach for AoR haemodynamics was utilized to provide a link between time-related 3D deformation and local haemodynamic conditions [1, 2]. Experimental data were used in order to establish real time 3D computed fluid dynamics models of David and

Yacoub AoR to evaluate and compare the impact of the surgical procedure on local shear stress and pressure profile.

MATERIALS AND METHODS

The methodology has been previously described in detail [1]. A brief description is provided here.

Animal protocol

The research protocol was approved by the Committee on Animal Care, Office Vétérinaire Cantonal, Lausanne, Switzerland. The *Principles of Laboratory Animal Care* formulated by the National Society for Medical Research and the *Guide for the Care and Use of Laboratory Animals* prepared by the National Academy of Sciences and published by the National Institutes of Health, NIH Publication No. 80–23, revised 1985, were applied for all animals. Each procedure, Yacoub or David, was performed on five domestic pigs, for a total of ten pigs (veterinary office, in regards to the applied statistical methodology (power 90%, $P < 0.05$,) allocated five animals in each group). After general anaesthesia was completed, monitoring was obtained in the following manner: central venous pressure by jugular venous catheter, invasive arterial pressure by femoral arterial catheter and five-lead ECG [1].

Activated clotting time > 480 s, in terms of systemic heparinization, was used throughout the procedure. Cardiopulmonary bypass was established by using a 32Fr venous cannula (SmartCannula®, Lausanne, Switzerland) in the right atrium and 20Fr cannula (Eopa® cannula, Medtronic Inc., Minneapolis, USA) in the aortic arch. After cross clamping, cardiac arrest was obtained by administration of anterograde cold crystalloid cardioplegia. The ascending aorta was opened transversely a few inches superior to the sinotubular junction (STJ) [1].

The Yacoub procedure was performed on five animals (mean weight 59.43 ± 3.33 kg, mean body surface 1.35 ± 0.13 m^2). The procedure and its details are mentioned elsewhere [3, 4]. Briefly, following dissection of the AoR from the surrounding tissue, the three sinuses of Valsava were removed. Graft (Gelweave, Vascutek Terumo, UK) size was determined as suggested by David [7]. Namely, after three sinuses were excised; the three commissures were pulled up in in straight manner. The diameter at the level of three commissures was determined by using the size for the stentless biological aortic valves. Subsequently, AoR reconstruction was performed according to the original report published by Yacoub *et al.* [3].

The David I procedure was also performed on five domestic pigs (mean weight 58.25 ± 4.84 kg, body surface of 1.37 ± 0.09 m2). The technique of aortic valve reimplantation into a straight graft has been described previously [7, 8].

In each AoR modality six 2 mm Sonometric Crystals (200 Hz, Sonometrics Corp, London, Ontario, Canada) were implanted. The crystal positions were as follows: at three commissures and their projection at the AoR base (Fig. 1). The basal spot is considered as the deepest point of each individual intervalvular triangle (IVT). The mentioned crystal arrangement corresponds to key landmarks of the geometrical 3D model of an AoR [9, 10]. Subsequently, interconnection of the key landmarks results in a triangular prism as a geometrical shape [1, 2, 9, 10]. High-fidelity catheter-tipped pressure transducers (Millar Instruments, Houston, USA) in the ascending aorta and left ventricle, served as invasive pressure measures. Flow at the ascending aorta was measured by a PeriVascular flow probe (Medistim ASA, Norway, Oslo) [1].

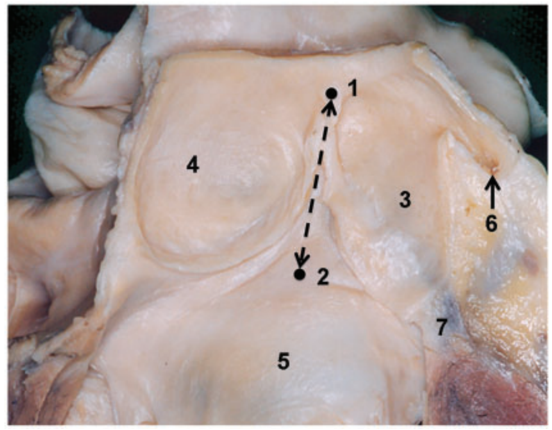

Figure 1: Dry dissected specimen of the AoR. The left and right coronary sinuses are seen in frontal plane. Two black dots mark the position of the commissural and basal crystal. The dashed double arrow indicates the vertically measured distance between two crystals. Note the topography between the anterior mitral valve leaflet and AoR base. 1.Commisural crystal, 2 AoR base crystal, 3. Left coronary sinus, 4.Non coronary sinus, 5. Anterior leaflet of the mitrla valve, 6. Left coronary artery and 7. Left fibrous body.

After stable haemodynamic conditions were achieved, animals were weaned from cardiopulmonary bypass. Under stable haemodynamic conditions, 10 consecutive heartbeats were analysed with registration of distances between individual crystals, of flow and of the pressure in the left ventricle and ascending aorta. Valve competence was verified by transoesophageal echoradioagraphy. At the end of the experiment, the heart was explanted and an autopsy was performed to confirm correct positioning for all six crystals [1].

Time- and pressure-related aortic root deformation

As defined previously according to cardiac cycle: time- and pressure- (pressure in the left ventricle and ascending aorta) related AoR 3-D geometries are defined as: (i) at the end of diastole and at the beginning of the isovolemic contraction when the pressure in the left ventricle starts to rise, (ii) aortic valve opening at equalization of arterial and ventricular pressure, (iii) peak ejection, (iv) end of the systole, when the aortic valve closes and at (v) the end of the isovolemic relaxation at the lowest pressure value in the left ventricle when the mitral valve opens [1].

Continuously registered distances between individual spots (crystals) at three commissures and their projection at the AoR base and measured pressure (in ascending aorta and left ventricle) were synchronized by using customized Sonometric system software (Sonometric Corporation). In data processing (CardioSoft program, Sonometric Corporation), time- and pressure-related data following crystal distances were evaluated (i) at the distance between each commissure at the horizontal level, (ii) the distance between crystals at the base of each IVT, (iii) the distance corresponding to each individual IVT and (iv) the diagonal distances between commissure and IVT base, corresponding to diagonal deformation of each individual AoR sinus [1].

The radius of the AoR base and of the STJ was calculated in accordance to Euclidian space where the relation between the isosceles triangle and the circumscribed circle [1, 12] were considered. The three crystals in the horizontal plane at the STJ and at the AoR base define an isosceles triangle [1, 11]. To note, the superior triangle placed at the STJ is defined by the three commissures. The inferior triangle positioned at the AoR base is defined by the three basal points of each individual IVT

Aortic root tilt and torsion angle

Due to the natural asymmetry of the AoR, the triangle at the STJ and AoR base are not parallel [9, 10]. The tilt angle of the AoR is defined as the angle between the plane of the STJ and plane of the AoR base. Positioning the geometrical model of the AoR into a x-y-z Cartesian coordinate system (CCS) [9, 10], with origin (0, 0, 0) in the middle and the deepest point of the non-coronary sinus (NCS) reflects that the AoR tilt angle is the angle between the triangle at the STJ and the triangle at the AoR base. Torsion displacement of the AoR was considered as horizontal displacement of the STJ over the AoR base. This is defined as rotation of the prism between the z-axis of CCS and the normal vector of the AoR base and the STJ [1].

Monte-Carlo simulation was used to avoid errors from measurements and angle calculations. Each measured parameter between the determined spot corresponding to the prism was drawn from a Gaussian distribution with a sample mean and variance (based on repeated measures of each segment). The prism was reconstructed on the basis of the drawn segments and the angles were computed for the reconstructed prism. The process was repeated 1000 times, and as such, having 1000 values of the torsion and the tilt angle for each prism, allowed us to generate a good statistical estimate of these quantities as described [1].

Statistical analysis of measured data

From each registered sequence, under stable haemodynamic conditions, 10 consecutive heartbeats were analysed. Data are presented as mean and standard deviation (Mean ± standard deviation). Statistical analysis was performed by using SciPy 0.18.0 (PSF scientific library, Delaware USA). Measured parameters, during the cardiac cycle, were tested for significance using the one-sided and/or two-sided *t*-tests. For both the AoR base and the STJ, three null hypotheses were tested (i) we assumed that the mean distance of left coronary sinus (LCS) and of the right coronary sinus (RCS) were equal (H01) (two-sided *t*-test), (ii) that the mean distance of LCS was smaller or equal to NCS (H02) and (iii) that the mean distance of RCS was smaller or equal to NCS (H03), (one-sided *t*-test). To test the hypothesis, the mean values of the intercommissural as well of the basal distances were compared at defined cardiac cycle time points. A P-value < 0.05 would reject the hypothesis.

The radius at the STJ and AoR base level was additionally evaluated as relative expansion, and values were compared to the baseline radius at the end of diastole [1].

Computational fluid dynamics modelling of the aortic root

Local pressure, velocity and shear stress profiles of the Yacoub and David AoR were evaluated in the computational fluid dynamics (CFD) simulation. The corresponding 3D geometry was established based on spatial time and pressure related AoR deformation.

At a defined time setting for the cardiac cycle, for both David and Yacoub AoR modalities, dimensions of the three-sided prism (as defined by six sonomicrometric crystals) were used to create time and pressure related geometrical deformations of the AoR.

As mentioned previously [1], a discretized set of 100 geometrical models was interpolated and generated in order to reproduce the geometrical deformation of the AoR and the movement of the three leaflets during the complete cardiac cycle. The ANSYS ICEMCFD (ANSYS Inc., Pennsylvania, USA) pre-processor tool was used to generate the multi-block structured grids needed by the Navier-Stokes Multi Block (NSMB) flow solver. An O-grid topology which aligns the hexahedral cells of the structured grid with the walls of the geometrical model) was employed to refine the mesh close to the walls in order to correctly capture the laminar boundary layer in these regions [12]. The grid for the AoR comprises 308 structured blocks for around 1.8 million cells.

Blood was modelled as a Newtonian fluid with a viscosity of 4.10^{-3} Pa.s and a density of 1060 kg/m^3. On the AoR wall, and on three leaflets, no-slip boundary conditions were imposed. Pulsatile velocity flow profile, pressure at the left ventricle and the ascending aorta pressure were applied according to measured values from the experimental scenario. The NSMB solver uses a cell-centred finite volume method to solve the compressible Navier-Stokes equations [12, 13]. The spatial discretization was ensured by a fourth order central scheme, while the time discretization was resolved by an implicit scheme [1].

RESULTS

AoR reconstruction and valve reimplantation were successfully performed. The registered mean radius at the SJ in the David group was 8.63 ± 0.29 mm and in the Yacoub group was 7.86 ± 0.08 mm, consequently oversizing the diameter of the SJ by 2 mm with a graft size of 20 mm (Gelweave, Vascutek Terumo, UK) in all 10 animals ($n = 5$ for Yacoub and $n = 5$ for David procedure).

Prism and definition of aortic root 3D deformation

In David and Yacoub AoR, expansion of the left LCS and right RCS was with some exceptions similar over the whole cardiac cycle. Parameters measured for LCS and in RCS were larger as compared distances measured at the NCS (Table 1).

In the Yacoub AoR, the calculated radius at the AoR base was larger than the radius at the SJ. The radius is expressed as a relative value. The value at the end of diastole was used as a baseline. Maximal expansion noted at peak ejection was 3.60 ± 1.44% for AoR base and 3.06 ± 1.40% for STJ, with minimal expansion at the end of isovolemic contraction at 0.30 ± 0.45% for the AoR base and 0.06 ± 0.14% for the STJ.

In David AoR, the radius expansion at the AoR base and at STJ was as follows: maximal expansion at peak ejection 1.58 ± 0.95% for the AoR base and 2.91 ± 1.75% for the STJ. Minimal expansion was registered at the end of diastole and was 0.17 ± 0.33% for the AoR base and 0.14 ± 0.51% for the STJ (Fig. 2).

In Yacoub AoR, the tilt and torsion angle showed the following pattern. The maximal value was registered at peak ejection: 23.94 ± 1.10° for tilt and 15.84 ± 0.98° for the rotation angle and

Table 1: Showing measured distances at the three commissures and at the AoR base, for David and Yacoub AoRs. (i) H01 (null hypothesis) assumed that LCS = RCS, (ii) H02 assumed that LCS < = NCS, (iii) H03 assumed that RCS < = NCS

	Intercommisural distance (mm) David AoR					
	LCS	RCS	NCS	*P* for H01	*P* for H02	*P* for H03
ED	15.97±0.07	14.67±0.54	12.62±1.11	0.064	*P* < 0.001	*P* < 0.001
Min	15.98±0.04	14.96±1.61	12.61±1.11	0.039	*P* < 0.001	*P* < 0.001
MaxE	16.25±1.24	15.09±1.61	13.14±0.92	*P* < 0.001	*P* < 0.001	*P* < 0.001
ES	16.2 ± 1.03	15.08±1.73	13.11±0.94	*P* < 0.001	*P* < 0.001	*P* < 0.001
Mid-D	16.05±1.09	14.89±1.61	13.11±0.94	0.033	*P* < 0.001	*P* < 0.001
	Distance at the AoR base (mm) David AoR					
ED	15.76±0.06	14.48±0.89	12.03±0.12	*P*<0.001	*P*<0.001	*P* < 0.001
Min	15.76±0.98	14.52±0.92	12.02±0.92	0.001	*P*<0.001	*P* < 0.001
MaxE	15.99±0.11	14.85±0.87	12.15±0.99	*P* < 0.001	*P* < 0.001	0.19
ES	15.93±0.13	14.87±0.93	12.17±0.90	*P*<0.001	*P* < 0.001	0.19
Mid-D	15.49±0.91	14.44±0.83	12.09±0.87	0.038	*P* < 0.001	*P* < 0.001
	Intercommisural distance (mm) Yacoub AoR					
	LCS	RCS	NCS	*P* for H01	*P* for H02	*P* for H03
ED	13.83±0.89	13.81±0.91	12.36±0.71	*P*<0.001	0.16	0.16
Min	13.80±0.90	13.83±0.91	12.39±0.71	*P*<0.001	0.16	0.16
MaxE	14.31±0.61	14.30±0.61	13.06±0.82	*P*<0.001	0.16	0.16
ES	14.32±0.55	14.30±0.62	13.20±0.07	*P*<0.001	0.16	0.16
Mid-D	13.91±0.91	13.85±0.91	12.45±1.68	*P*<0.001	0.16	0.16
	Distance at the AoR base (mm) Yacoub AoR					
ED	14.23±0.08	14.41±0.82	13.47±0.10	*P*<0.001	0.16	*P*<0.001
Min	14.30±0.07	14.44±0.82	13.65±0.05	*P*<0.001	0.16	*P*<0.001
MaxE	14.50±0.23	14.80±0.60	14.03±0.11	*P*<0.001	0.19	0.0017
ES	14.47±0.22	14.78±0.81	14.02±0.20	0.26	0.17	0.001
Mid-D	14.20±0.18	14.30±0.60	13.43±0.95	*P*<0.001	0.16	*P*<0.001

LCS: left coronary sinus; RCS: right coronary sinus; NCS: non-coronary sinus; ED: end diastole; Min: end of the isovolemic contraction; Max: maximal/peak ejection; ES: end of systole; Mid-D: mid-term of diastole at mitral valve opening; H0: null hypothesis.

at aortic valve closure it was 24.01 ± 1.08° for tilt and 16.04 ± 0.53° for rotation angle. From here on the rotation and tilt angle decreased and reached its minimal value at the end of diastole with 22.21 ± 1.05° tilt and 14.10 ± 0.63° rotation angle (Fig. 3). From mid diastole, both angles did not change tremendously. A very similar pattern was observed in David AoR. Tilt and rotation angle increases from the end of isvolemic contraction to peak ejection and was 23.70 ± 1.49° for tilt and 25.81 ± 0.73° for rotation angle. At closure of the aortic valve, the tilt angle was 23.51 ± 1.47° and torsion angle was 25.63 ± 0.73°. From here on the tilt and rotation angle dropped and at closure of the mitral valve were 21.31 ± 0.80° and 23.62± 0.62°, respectively (Fig. 3).

Computational fluid dynamics of native versus David aortic root

Using the mentioned geometrical results as well as the measured *in situ* parameters such as pressure and flow, CFD modelling for Yacoub and David AoR were established in order to evaluate local shear stress and the pressure pattern on AoR components.

Shear stress profile

At the end of diastole at the three-leaflet body, the valve hinge area, as well at the IVTs, had low shear stress in a range of 0–10 Pa, which was found in Yacoub as well in David AoR. In David AoR, the leaflet cooaptation was in high shear stress > 100 Pa, whereas in Yacoub AoR it ranged from a moderate 40 Pa to high 100 Pa shear stress. At the end of isovolemic contraction, there was shear stress augmentation in both AoR geometries. The leaflet body, their attachment and the IVTs registered low 0–10 Pa to moderate 20–40 Pa shear stress. Moderate shear stress was more pronounced in David AoR, whereas in Yacoub AoR there was a predominance of low shear stress (0–10 Pa). The leaflet cooaptation in David AoR was a high > 100 Pa and in Yacoub AoR it ranged from moderate 40 Pa to a high 100 Pa of shear stress (Fig. 4, Video 1).

At peak ejection, the following was noticed in YacoubAoR, the leaflet body registered moderate shear stress in a range of 30–60 Pa. The superior 2/3 of the IVT registered moderate shear stress ranging from 30 to 60 Pa, whereas the basal 1/3 had a low shear stress range of 0–10 Pa. The three commissures registered in a high shear stress area > 100 Pa, whereas at the cooaptation regions shear stress ranged from a moderate 40 Pa to a high of 100 Pa. In David root, the superior 1/2 of the leaflet body was at high shear stress > 100 Pa, and the inferior 1/2 showed moderate to high shear stress ranging from 30 to 80 Pa. The superior part of the IVT and the commissures had high shear stress at > 100 Pa, whereas the inferior 3/4 registered moderate to high shear stress from 30 to 80 Pa. Cooaptation was at a moderate shear stress ranging from 30to 50 Pa to a high shear stress > 100 Pa.

At aortic valve closure in YacoubAoR, the leaflet body, valve attachment, the IVTs were exposed to low shear stress of 0–10 Pa and a moderate 10–40 Pa. Cooaptation at its central part registered high shear stress at > 100 Pa and its lateral segment had moderate from 20 to 40 Pa shear stress. In David AoR, the

EXPERIMENTAL

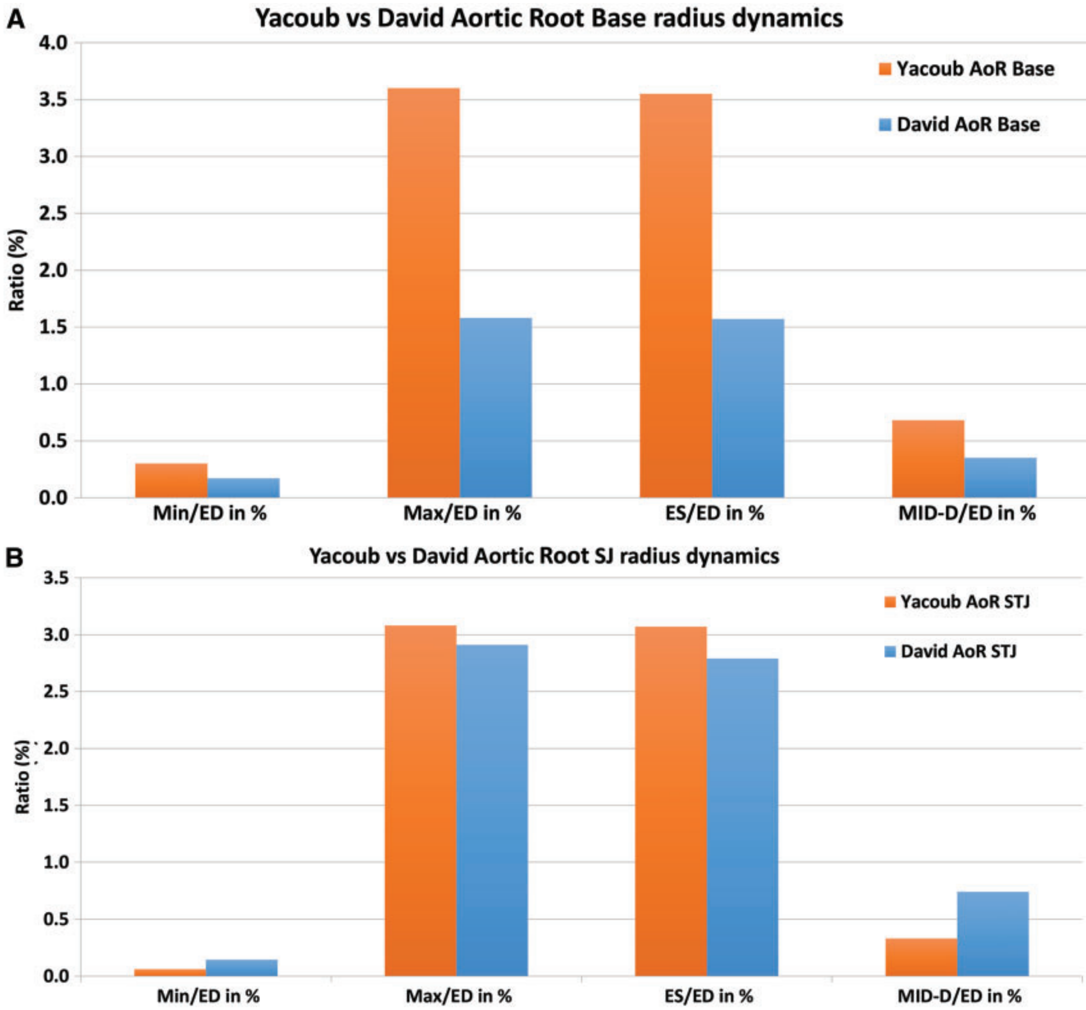

Figure 2: Comparison of the relative radius changes at the STJ (**A**) and at the AoR base (**B**) and in Yacoub versus David AoR. The radius at the end of diastole was considered the baseline value. STJ: sinotubular junction; LCS: left coronary sinus; RCS: right coronary sinus; NCS: non-coronary sinus; ED: end diastole; Min: end of the isovolemic contraction; Max: maximal/peak ejection; ES: end of systole; Mid-D: mid-term of diastole at mitral valve opening.

leaflet body, their attachment and the IVTs were similarly exposed to low shearstress at 0–10 Pa and moderate stress of 10–40 Pa. Cooaptation was registered high shear stress > 100 Pa (Fig. 4, Video 1).

Pressure profile

In YacoubAoR at the end of diastole, the leaflet body, the three IVTs and the leaflet nadirs were in moderately elevated pressure 90–110 mmHg, cooaptation was in a low to moderate pressure field of 70–100 mmHg. In David AoR, the leaflet cooaptation was exposed to a low to moderate pressure range from 70 to 10 mmHg where the leaflet body, the three IVTs and the leaflet nadirs were in a high pressure area > 140 mmHg (Fig. 5, Video 2).

At the end of the isovolemic contraction in YacoubAoR, the valves and the valve nadirs were in a moderate pressure range from 90 to 100 mmHg, whereas the IVTs were in a high pressure range > 140 mmHg. In contrast, in David AoR the valves, nadirs as well the IVTs were in an extremely high pressure range of > 150 mmHg. At the same time frame, valve cooaptation in both geometries was in a low to moderate pressure field of 70–100 mmHg (Fig. 5, Video 2).

At peak ejection, in Yacoub AoR, the leaflet body, the three IVTs and the leaflet nadirs registered low to moderately elevated pressure at a 70–100 mmHg range, whereas cooaptation of leaflets was in a low pressure field < 70 mmHg. In David AoR, the inferior 1/2 of the leaflet body, the three IVTs and the leaflet nadirs were in a high pressure range > 150 mmHg where the superior 1/2 was exposed to a pressure range of between 90 to 120 mmHg. Cooaptation in this geometry was also in a low to moderate pressure field of 70–100 mmHg. At the end of systole, that is at aortic valve closure, the following was noticed: in the Yacoub AoR leaflet body, the three IVTs, and the leaflet nadirs registered a low pressure > 90 mmHg range, while in David AoR these structures had a moderate high pressure field of 100–130 mmHg. The cooaptation in both AoR modalities was in a low pressure range > 70 mmHg (Fig. 5, Video 2).

DISCUSSION

Local haemodynamic parameters such as shear stress and pressure distribution over AoR elements in Yacoub AoR have a more favourable pattern as compared to David AoR. In David AoR, high pressure (> 130 mmHg) accompanied by low shear stress

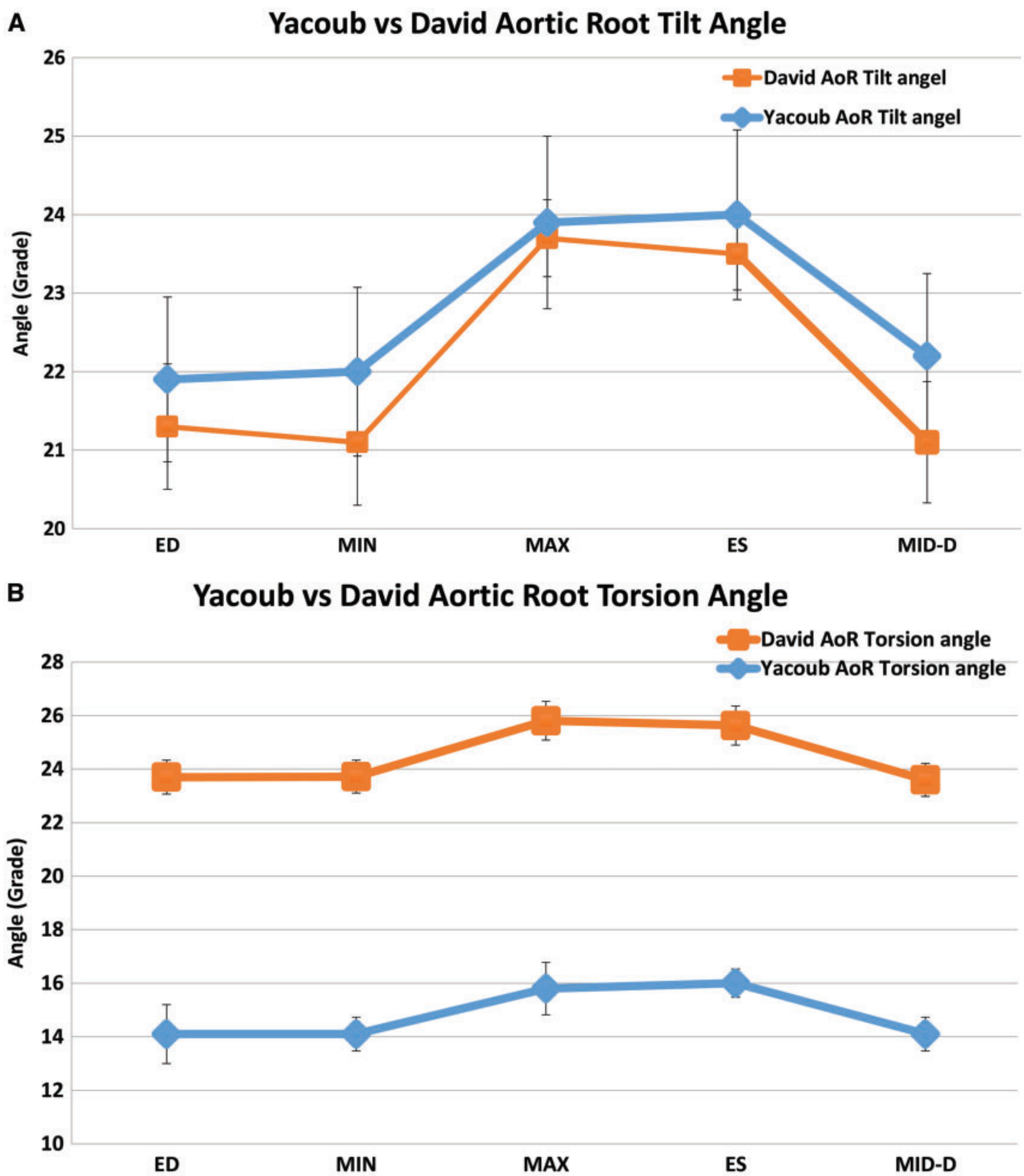

Figure 3: Tilt (**A**) and rotation (**B**) angle as calculated for Yacoub and David AoR. Maximal tilt angle and rotation angle in both root modalities were registered at peak ejection and closure of the aortic valve. Minimal rotation and tilt angle were observed at the phase of diastole.(data are presented as Mean ± SD, error bars represent the standard deviation), ED: end diastole; Min: end of the isovolemic contraction; Max: maximal/peak ejection; ES: end of systole; Mid-D: mid-term of diastole at mitral valve opening; SD: standard deviation.

(range 0–10 Pa) was registered at three leaflets, IVTs, valve nadirs and commissures from the period of aortic valve closure to the end of isovolemic contraction. In contrast, in Yacoub AoR, similar pressure and shear stress conditions were present only for a short period of isovolemic contraction. Interestingly, leaflet cooaptation in both numerical simulations during the whole cardiac cycle was exposed to moderate pressure and high shear stress (> 100 Pa).

AoR morphology and consequently its function are complex. The shape of the AoR components follows a well-defined morphological pattern. This natural AoR asymmetry may be defined by a simple geometrical object, such as a three-sided prism [9, 10]. It is logical that a well-defined 3D architecture plays an important role in normal AoR function. In our previous work, we showed that the interaction of AoR elements during a cardiac cycle followed a well-defined, very precise, and repetitive shape deformation. From a haemodynamical point of view the relation of the AoR to the LVOT is of crucial importance. During the short period of systole, the AoR takes on a cylinder-like shape, and is aligned in a straight line with the LVOT and ascending aorta. This alignment achieves a reduction of tissue stress and resistance during the ejection phase. At this point, the complex 3D time-related AoR deformation may be determined by two numerical parameters: AoR rotation and tilt angle [1, 2].

The mentioned geometrical approach was used to compare 3D time- related deformation of the AoR following a David or Yacoub procedure and to evaluate the impact of synthetic elements on local haemodynamic conditions. This allowed us to

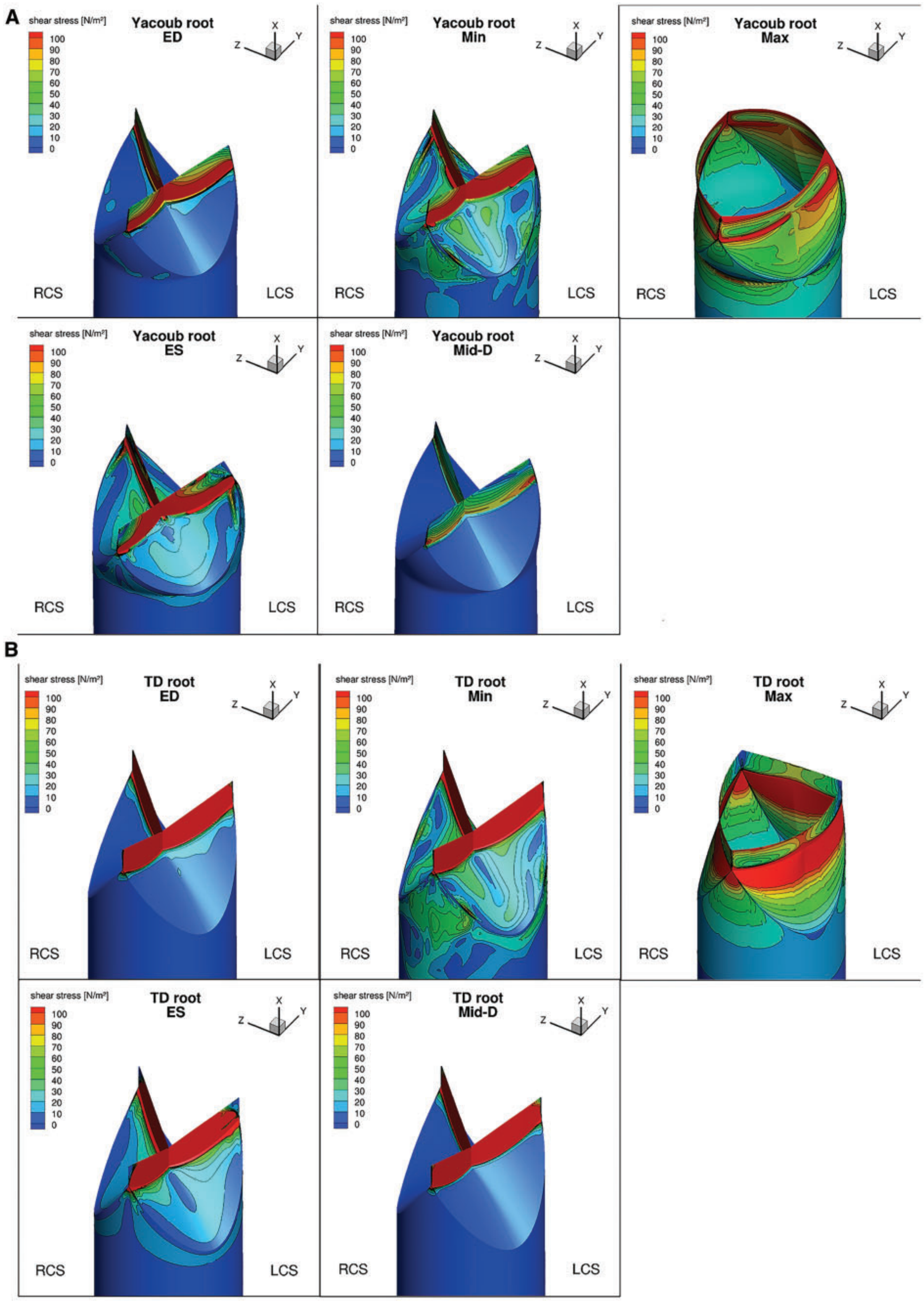

Figure 4: Shear stress profile at leaflets, IVTs, the cooaptations and valve attachment in Yacoub (**A**) and David (**B**) AoR. ED: end diastole; Min: end of the isovolemic contraction; Max: maximal/peak ejection; ES: end of systole; Mid-D: mid-term of diastole at mitral valve opening.

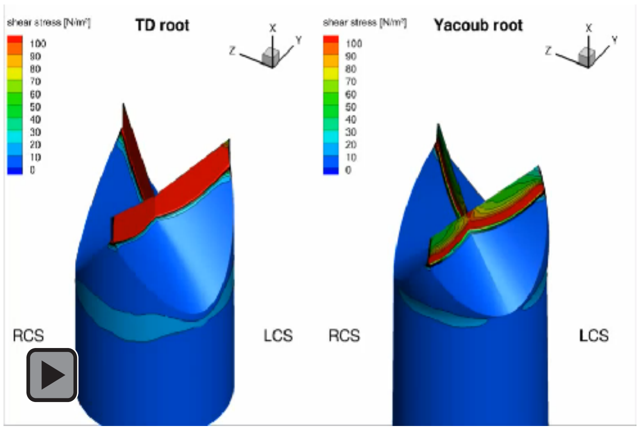

Video 1: Shear stress dynamics in Yacoub and David AoR during the cardiac cycle.

objectively evaluate the impact of these two most commonly used reconstructive procedures on AoR haemodynamics.

Following Yacoub as well as the David procedure, AoR sinuses were replaced by a synthetic graft. In the first case, neo-sinuses are created and the AoR base stands alone without any structural support, whereas the commissures, the superior segment of the IVTs as well the STJ are supported by the graft. In comparison, in the David procedure the aortic valve is reimplanted into a straight tube, while the AoR base, IVTs and STJ are surrounded by the graft material [7, 8].

The rotation and tilt angle describing global AoR geometrical deformation during the cardiac cycle in both investigated geometries demonstrates a very similar pattern. The 3D geometry in Yacoub and David AoR at diastole had a cylinder-like architecture where the levels of the STJ and of the AoR base are not parallel to each other. The rotation as well as the tilt angle in both AoR formations increased to the maximum value at ejection and decreased to its minimal value at the end of isovolemic relaxation. In both cases, AoR changed from a straight cylinder at diastole to a more twisted cylinder-like structure at ejection. The tilt angle increase as observed in Yacoub and David AoR at ejection will bring the STJ into a more tilted relationship to the AoR base, and as a result the AoR will enclose an augmented angle with the LVOT during ejection, as occurs during diastole. At this point we have to note that in native AoR, an opposite phenomenon occurs, where both the tilt and rotation angle reach their minimal value at ejection and maximal values at diastole. This decrease of both angle positions at the AoR results in an almost a straight line with the LVOT tract and ascending aorta [1, 2].

Considering the mentioned 3D deformation pattern registered in David and Yacoub AoR, one would expect similar, but definitively less favourable haemodynamic conditions as compared to native AoR. In native AoR, elevated pressure and low shear stress were registered only during the short period of the isovolemic contraction. In contrast, in David AoR, low shear stress and high pressure were registered over two-third of the period of the cardiac cycle. In regards to similar changes of AoR tilt and rotation angle in the David and Yacoub AoR, it would be logical to obtain similar results in CFD simulation. However, this was not the case. In Yacoub AoR, low shear stress conjoined with high pressure was registered only at the end of the isovolemic contraction as in native AoR.

According to our results, the divergence of the shear stress and pressure profiles in David and Yacoub geometries is very clear. This phenomenon can probably be explained by more than one reason. For example, it is quite certain that the role of the neo sinuses should not be neglected, however, this has not been evaluated in recent reports and may be considered as a task for future research. Moreover, the AoR base in Yacoub root as compared to the David AoR is not included in any form into the graft and as such it preserves its natural compliance. The preservation of natural compliance may explain the maintenance of the almost natural dynamic between the AoR base and STJ. Namely, in native AoR the radius of the base is about 5–10% larger than the radius of the STJ and this relation is preserved through the whole cardiac cycle [14, 15]. The same relation between AoR base and STJ is also preserved in Yacoub AoR and may be one of the key elements providing better physiological conditions in the AoR [3, 5, 6].

According to these experimental observations, one would expect that the Yacoub procedure is state-of-the-art for AoR reconstruction. In fact, however, the David procedure has excellent results and is increasingly accepted in the surgical community as the most appropriate procedure in young- and middle-aged adults having dilatation of the AoR. Long-term results that include a considerable number of cases indicate excellent outcome with freedom for valve/cusp related reintervention in the long term that is superior to 90% [14, 15]. The long-term results for the Yacoub procedure are not as excellent, and the reoperation rate because of valve durability in the midterm is 17% [5, 6, 16, 17]. This is due to the significant prevalence of important valve regurgitation during the short/mid term that may be as high as 22% [17].

It appears that the haemodynamic advantage of the Yacoub geometry presented in this report loses its impact in clinical reality. The structural reason for progressive aortic valve insufficiency is due to early as well as late dilatation of the AoR base. On the one hand, it is clear that the AoR base is not implanted into a rigid graft that would provide structural stabilization and at the same time prevent annulus dilatation. On the other hand, in patients with malformations such as Marfan syndrome, the tissue weakening and consequent annulus dilatation reflect the natural course of the disease progression. Further, in our Yacoub AoR simulation of the local pressure profile at the root base registered an elevated pressure (> 120 mmHg) during the whole period of diastole. Clearly in AoR base with weakened connective tissue, the elevated pressure combined with an absence of synthetic support definitively does not prevent annulus dilatation and consequent malfunction of the three leaflets.

Limitations of the study

This was an experimental study and the results obtained may not be completely interpreted into daily clinical practice. Additionally, the acute nature of the experiments does not address haemodynamic conditions in both AoR modalities over the long term, which needs to be definitively addressed in future research. Additionally, the surgical procedures were performed on healthy AoR and as such do clearly not correspond to a real world setting. Further the human and pig AoR do not have the same anatomy, which is substantially marked by a larger muscular bridge between non and right coronary sinus. However, both AoR morphologies are similar enough to translate the obtained haemodynamical results to a real clinical scenario. Additionally, it would be interesting to explore the effect of AoR base annuloplasty (CAVIAAR

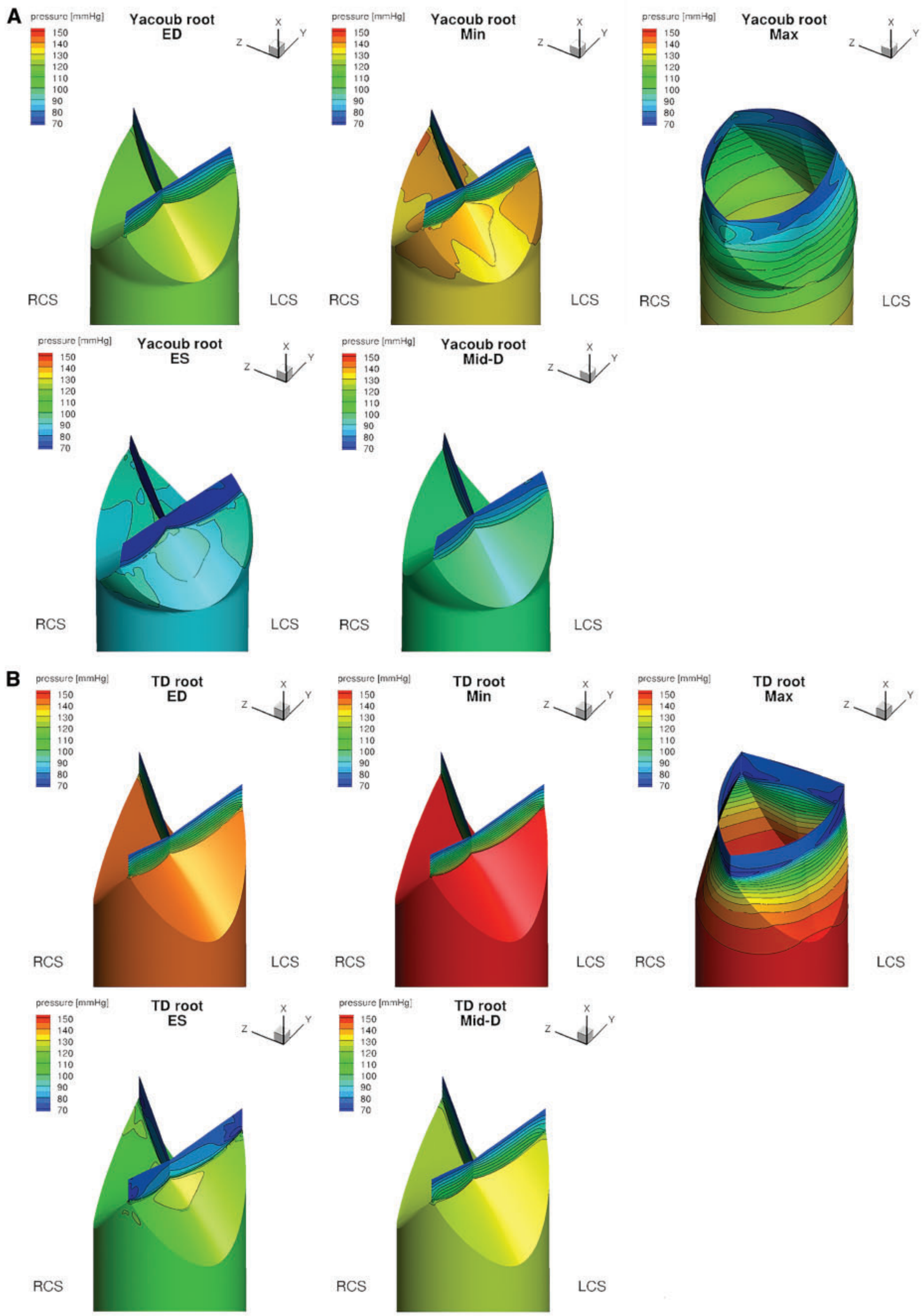

Figure 5: Pressure profile at leaflets, IVTs, the cooaptations and valve attachment in Yacoub (**A**) and David (**B**) AoR. ED: end diastole; Min: end of the isovolemic contraction; Max: maximal/peak ejection; ES: end of systole; Mid-D: mid-term of diastole at mitral valve opening.

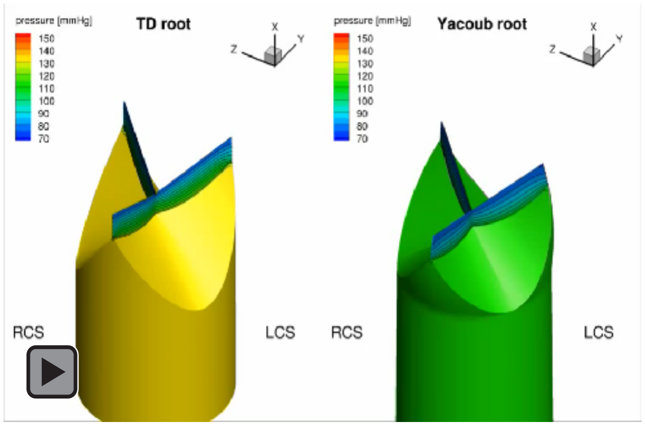

Video 2: Pressure dynamics in Yacoub and David AoR during the cardiac cycle.

technique) on AoR haemodynamics. This technique provides AoR base stabilization in root reconstruction, although the promising short-term results are still unclear over the mid-term as well the long-term [18, 19]. On the other hand, one may argue why the 'more physiological' Valsava Graft was not used. This may be explained with two facts, using the straight graft in David I, the IVTs are reimplanted in a straight vertical manner, where the position mimics the natural morphology of the IVTs. Meanwhile, at the Valsava Graft, the IVTs follow the convex wall of the sinus, which may result in depressed leaflet cooaptation and may be responsible for late valve failure.

Funding

This work was supported by a research grant of the Swiss Heart Foundation, Bern, Switzerland. Principal Grant holder is Denis Berdajs.

Conflict of interest: none declared.

REFERENCES

[1] Berdajs D, Mosbahi S, Forro Z, Ferrari E, Charboniere D, von Segesser LK. Numerical analysis of the aortic root 3D morphology during cardiac cycle. Eur J Cardiothorac Surg 2016;49:1213–21.
[2] Berdajs D, Mosbahi S, Forro Z, Burki M, von Segesser LK. Aortic root hemodynamics following David procedure: numerical analysis of 3D hemodynamics. Eur J Cardiothorac Surg 2016;49:1588–98.
[3] Yacoub M, Faga n A, Stassano P, Radley-Smith R. Result of valve conserving operations for aortic regurgitation [abstract]. Circulation 1983;68(suppl): III321.
[4] David TE, Feindel CM. An aortic valve-sparing operation for patients with aortic incompetence and aneurysm of the ascending aorta. J Thorac Cardiovasc Surg 1992;103:617–21.
[5] Luciani GB, Casali G, Tomezzoli A, Mazzucco A. Recurrence of aortic insufficiency after aortic root remodeling with valve preservation. Ann Thorac Surg 1999;67:1849–52.
[6] Hanke T, Charitos EI, Stierle U, Robinson D, Gorski A, Sievers HH *et al.* Factors associated with the development of aortic valve regurgitation over time after two different techniques of valve-sparing aortic root surgery. J Thorac Cardiovasc Surg 2009;137:314–19.
[7] David TE. Aortic valve repair and aortic valve-sparing operations. J Thorac Cardiovasc Surg 2015;149:9–11.
[8] David TE. How I do aortic valve sparing operations to treat aortic root aneurysm. J Card Surg 2011;26:92–9.
[9] Berdajs D, Turina PL, Clinical M. Anatomy of the aortic root. Cardiovasc Surg 2002;10:320–7.
[10] Berdajs D, Zund G, Schurr U, Camenisch C, Turina MI, Genoni M. Geometric models of aortic and pulmonary roots: Suggestion for Ross procedure. Eur J Cardiothoracic Surg 2007;31:31–5.
[11] Whithwort WA. Triliniear coordinates and other methods of modern analytical geometry oft wo dimensions an elemntary treatist. Cornell 1866;206–19.
[12] Vos JB, Leyland P, van Kemenade V, Gacherieu C, Duquesne N, Lötstedt P. NSMB Handbook 6.07, March 2014:601–697
[13] Vos J, Rizzi A, Corjon A, Chaput E, Soinne E. Recent advances in aerodynamics inside the NSMB (Navier-Stokes Multi-Block) consortium. AIAA Paper 1998;802:1998–9.
[14] David TE. Aortic valve sparing operations: outcomes at 20 years. Ann Cardiothorac Surg 2013;2:24–9.
[15] Leontyev S, Trommer C, Subramanian S, Lehmann S, Dmitrieva Y, Misfeld M *et al.* The outcome after aortic valve-sparing (David) operation in 179 patients: a single-centre experience. Eur J Cardiothorac Surg 2012;42:261–6.
[16] Birks EJ, Webb C, Child A, Radley-Smith R, Yacoub MH. Early and long-term results of a valve-sparing operation for Marfan syndrome. Circulation 1999;100:II-29–II-35.
[17] de Oliveira NC, David TE, Ivanov J, Armstrong S, Eriksson MJ, Rakowski H *et al.* Results of surgery for aortic root aneurysm in patients with Marfan syndrome. J Thorac Cardiovasc Surg 2003;125:789–96.
[18] Lansac E, Bouchot O, Arnaud Crozat E, Hacini R, Doguet F, Demaria R *et al.* Standardized approach to valve repair using an expansible aortic ring versus mechanical Bentall: early outcomes of the CAVIAAR multicentric prospective cohort study. J Thorac Cardiovasc Surg 2015;149:37–45.
[19] Wuliya M, Sleilaty G, Di Centa I, Khelil N, Berrebi A, Czitrom D *et al.* An expansible aortic ring to preserve aortic root dynamics after aortic valve repair. Eur J Cardiothorac Surg 2015;47:482–90.

EXPERIMENTAL